Pervasive foreshock activity across southern California

Daniel T. Trugman[1], Zachary E. Ross[2]

[1] Geophysics Group, Earth and Environmental Sciences Division, Los Alamos National Laboratory, Los Alamos NM

[2]Seismological Laboratory, California Institute of Technology, Pasadena CA

Corresponding author: Daniel Trugman (dtrugman@lanl.gov)

Key Points:

- We analyze foreshock activity in a catalog of more than 1.8 million earthquakes in southern California.
- Foreshock occurrence significantly exceeds the background seismicity rate for 72% of candidate mainshocks.
- Durations of elevated foreshock activity range from days to weeks for these sequences.

Abstract

Foreshocks have been documented as preceding less than half of all mainshock earthquakes. These observations are difficult to reconcile with laboratory earthquake experiments and theoretical models of earthquake nucleation, which both suggest that foreshock activity should be nearly ubiquitous. Here we use a state-of-the-art, high-resolution earthquake catalog to study foreshock sequences of magnitude M4 and greater mainshocks in southern California from 2008-2017. This highly complete catalog provides a new opportunity to examine smaller magnitude precursory seismicity. Seventy-two percent of mainshocks within this catalog are preceded by foreshock activity that is significantly elevated compared to the local background seismicity rate. Foreshock sequences vary in duration from several days to weeks, with a median of 16.6 days. The results suggest that foreshock occurrence in nature is more prevalent than previously thought, and that our understanding of earthquake nucleation may improve in tandem with advances in our ability to detect small earthquakes.

Plain Language Summary

Earthquakes often occur without warning or detectable precursors. Here we use a new, highly complete earthquake catalog to show that most mainshock earthquakes in southern California are preceded by elevated seismicity rates – foreshocks – in the days and weeks leading up to the event. Many of these foreshock earthquakes are small in magnitude and hence were previously undetected by the seismic network. These observations help bridge the gap between observations of real earth fault systems and laboratory earthquake experiments, where foreshock occurrence is commonly observed.

1 Introduction

There has long been an underlying tension between two competing observations of earthquake occurrence. From one perspective, the occurrence of large earthquakes within a fault zone appears random in time, and indeed classical models of earthquake hazard are based on a Poisson process that encodes this random, memoryless behavior by assumption (Baker, 2013). In contrast, one of the most striking characteristics of earthquakes is that they tend to cluster in space and time, with the triggering of aftershocks following larger, mainshock earthquakes being the best-studied example. The physical mechanisms driving aftershock occurrence are reasonably well-understood, at least at a high level: slip on the mainshock fault interface imparts both static (King et al., 1994; Lin & Stein, 2004; Stein, 1999) and dynamic (Brodsky, 2006; Gomberg & Davis, 1996; Kilb et al., 2000; Velasco et al., 2008) stress changes in Earth's crust that trigger aftershock activity. Postseismic fault slip, subcrustal viscoelastic relaxation, and poroelastic stress transfer may also play an important role in certain circumstances (Freed, 2005; Freed & Lin, 2001; Koper et al., 2018; Ross et al., 2017).

Foreshocks – earthquake occurrences preceding mainshocks – are less well understood. While it is unambiguous that foreshocks do occasionally occur, both their physical significance and their relative prevalence are subject to vigorous debate (Ellsworth & Bulut, 2018; Seif et al., 2019; Shearer & Lin, 2009; Tape et al., 2018). In laboratory earthquake experiments, precursory slip events analogous to foreshocks are observed in nearly all instances (Bolton et al., 2019; Johnson et al., 2013; Rouet-Leduc et al., 2017; W. Goebel et al., 2013). Likewise, theoretical models of fault friction, including the widely used rate-and-state framework, typically require a seismic nucleation phase preceding dynamic rupture (Ampuero & Rubin, 2008; Dieterich, 1994; Marone, 1998). These facets of laboratory and theoretical earthquake behavior suggest that foreshock occurrence may be a natural manifestation of a nucleation or preslip process preceding rupture (Bouchon et al., 2013; Dodge et al., 1996). This interpretation if correct would have important scientific and practical consequences, and would intimate that foreshocks could potentially be used to forecast characteristics of eventual mainshock occurrence.

One problem with this interpretation is that foreshock activity in nature is not observed as frequently as it should be if it were a universal feature of earthquake nucleation. While it is notoriously difficult to compare different foreshock studies due to different magnitude thresholds or space-time selection windows (Reasenberg, 1999), foreshocks have previously been observed to precede 10-50% of mainshocks (Abercrombie & Mori, 1996; Chen & Shearer, 2016; Jones & Molnar, 1976; Marsan et al., 2014; Reasenberg, 1999). Taking these observations at face value, what happens during the nucleation process of the other 50 to 90% of earthquakes? Are there really no foreshocks, or are we simply not listening closely enough to detect them? The notion that there exists undetected but substantial foreshock activity is supported by a recent meta-analysis of 37 different studies of foreshocks (Mignan, 2014), which revealed systematic differences in the outcome depending on the minimum magnitude of foreshock detected. A similar effect can be seen in laboratory experiments, as the ability to forecast imminent laboratory earthquakes depends fundamentally on the magnitude of completion of precursory slip events (Lubbers et al., 2018).

In this study, we measure foreshock activity using a powerful new tool: a state-of-the-art earthquake catalog (Ross et al., 2019) of more than 1.81 million earthquakes that occurred in southern California from 2008 through 2017. The extraordinary detail of this catalog, which is complete regionally down to M0.3 and locally down M0.0 or less, allows us to examine precursory seismicity at the smallest of scales, in direct analog to well-recorded laboratory experiments. We find that elevated foreshock activity is pervasive in southern California, with 72% of earthquake sequences exhibiting a significant, local increase in seismicity rate preceding the mainshock event. The spatiotemporal evolution of these sequences is diverse in character, a fact which may preclude real-time forecasting based on foreshock activity. Nevertheless, these results help bridge the gap in our understanding of precursory activity from laboratory to Earth scales.

2 Earthquake Catalog Data

We analyze earthquake sequences in southern California derived from the Quake Template Matching (QTM) earthquake catalog (Ross et al., 2019). This recently released catalog of southern California seismicity from 2008 – 2017 was compiled using approximately 284,000 earthquakes listed in the Southern California Seismic Network (SCSN) catalog (Hutton et al., 2010) as templates for network-wide waveform cross-correlation (Gibbons & Ringdal, 2006; Shelly et al., 2007), yielding more than 1.81 million detected earthquakes. The vast majority of these newly detected earthquakes are small in magnitude ($-2 < M < 0$), well beneath the M1.7 completeness threshold of the original SCSN catalog. The QTM catalog, by contrast, is more than an order of magnitude more complete, with consistent detection at M0.0 and below in regions of dense station coverage.

We examine foreshock activity preceding magnitude M4 and greater mainshocks located within the latitude and longitude ranges of [32.68°, 36.20°] and [-118.80°, -115.40°]. This spatial boundary was guided by the density of the SCSN station coverage and the local magnitude of completeness (Figure S1), since in more remote locations the template matching detection threshold is poorer. The lower latitude boundary of 32.68° is set to approximate the California/Mexico border, so the study region only contains events within southern California.

Within this study region, we select a total of 46 mainshocks that are relatively isolated in space and time from other larger events, to ensure that the selected events are indeed mainshocks as traditionally defined, and that the seismicity rate during the pre-event window is not biased high due to aftershock triggering from unrelated events. To do this, we have excluded candidate mainshocks that occur nearby to and closely following another larger earthquake (Supplementary Text S1). The spatial and temporal extent of these exclusion windows increases with the magnitude of the larger earthquake in proportion to its expected rupture length (Wells & Coppersmith, 1994), but the key results of our analyses do not depend strongly on the details of this parameterization (Table S1). We note that this exclusion criteria removes a large number of potential mainshocks occurring in the months following the 2010 M7.2 El Mayor-Cucapah earthquake, when the high triggered seismicity rate (Hauksson et al., 2011; Meng & Peng, 2014) renders foreshock analyses problematic. The El Mayor-Cucapah event is not considered in this study due to its location in Baja California, to the south of our study region, though it was itself preceded by a notable foreshock sequence (Chen & Shearer, 2013).

3 Methods

For each selected mainshock, we measure the local background rate of seismicity within 10 km epicentral distance of the mainshock using the interevent time method (Hainzl et al., 2006). In this technique, the set of observed interevent time differences $\boldsymbol{\tau}$ between subsequent events, are modeled as gamma distribution:

$$\boldsymbol{p(\tau) = C \cdot \tau^{\gamma-1} \cdot e^{-\mu\,\tau}}. \qquad (1)$$

Here, μ is the background rate, γ is the fraction of the total events that are background events, and $\boldsymbol{C = \mu^{\gamma}/\Gamma}(\gamma)$ is a normalizing constant. The appeal of the interevent time method is that it can be used to extract a background rate from temporally clustered earthquake catalog data without assuming an explicit functional form for triggered, non-background seismicity as in the popular epidemic type aftershock sequence (ETAS) model (Ogata, 1988). For each earthquake, we solve for μ using a maximum likelihood approach (van Stiphout et al., 2012), and estimate uncertainties using a log-transformed jackknife procedure (Efron & Stein, 1981).

Having established the local background rate, we consider potential foreshocks within this same 10 km distance range from the mainshock. While most previous studies neglect the local background rate and consider any earthquake sufficiently close in space and time to the mainshock to be a foreshock (Abercrombie & Mori, 1996; Chen & Shearer, 2016), this assumption is clearly problematic for the QTM catalog due to its high spatiotemporal event density. Thus, to measure the statistical significance of foreshock activity, we take a probabilistic approach in which we first count the observed number of earthquakes N in the 20 days preceding the mainshock, and then use Monte Carlo simulations to compute the probability p of observing at least N events during the 20-day / 10-km window, given the background rate $\boldsymbol{\mu}$ and its uncertainty. Low p-values are indicative of foreshock activity rates in excess of the background rate, and we consider $p < 0.01$ to be statistically significant evidence for elevated foreshock activity. We note that this probabilistic definition of a foreshock differs from the deterministic approach used in previous studies, but as we show below, our approach gives comparable results.

These background rate estimates, when combined with the relative completeness of the QTM catalog, enable measurement of the duration of significant foreshock activity, a subject that has not been carefully studied to date. To do this, we calculate the event rate within 5-day moving windows (and the same 10 km spatial windows). We work backwards in time from the mainshock origin time $T = 0$, in steps of 0.1 days, until the observed event rate falls to within one standard deviation of the background rate $\boldsymbol{\mu}$, and take the window end time to be the duration estimate. We use a 5-day window (rather than, for example, 10 days or 20 days), as we found it to be the best compromise between precision in defining the onset of foreshock sequences, and robustness to short-duration gaps in seismicity. Measurement uncertainties in the duration estimates are of order 1 day, controlled primarily by the uncertainty in the background rate and the temporal averaging (5 days) used to compute the observed event rates.

It is also important to understand how improved catalog completeness augments our understanding of foreshock sequences. This issue is pertinent both within and beyond the study region of California, as future studies in regions across the globe will provide new high-resolution catalogs by applying advanced event detection techniques (Kong et al., 2019; Yoon et al., 2015). To address this question in southern California, we repeat our analysis of the 46 foreshock sequences using the SCSN catalog instead of the QTM catalog (Figure S2), with an identical procedure to calculate background rates and compute the p-value of the observed foreshock count within 20 days and 10 km.

4 Results

In total, 33 out 46 mainshocks in southern California have a statistically significant increase in foreshock activity relative to the background seismicity rate (Figure 1 and Table S2). This 72% fraction suggests that precursory seismicity is more ubiquitous than previously understood, and that the discrepancy between the prevalence of foreshocks in laboratory and real Earth studies may in part be explained by observation limitations. This hypothesis is supported through direct comparison with the SCSN catalog, in which only 22 of the 46 sequences exhibit significant foreshock activity. This fraction is consistent with recent studies of foreshocks in California (Chen & Shearer, 2016), which helps validate our methodology that invokes a probabilistic definition of foreshock activity instead of a deterministic one.

The improvement in the resolution of foreshock sequences using the QTM catalog is particularly notable given that the SCSN catalog, with a nominal magnitude of completeness of M1.7, is among the highest quality network-based catalogs currently available. Despite this, there are numerous cases in which the SCSN catalog misses foreshock sequences nearly in their entirety (Figure S3), with the 2014 M5.1 La Habra earthquake providing an illustrative example (Figure 2). In other instances where foreshock activity is apparent in both catalogs, the QTM catalog provides improved detail of the low-magnitude foreshock events that provide a more complete perspective of the nucleation process. For example, in the earthquake sequences depicted in Figure 3, the precise timing of the onset of each sequence is readily apparent using the QTM catalog, but is impossible to discern using the SCSN catalog alone.

The QTM catalog also provides a unique opportunity to examine the spatial and temporal characteristics of foreshock sequences in southern California. We can, for example, estimate the duration of foreshock activity by measuring the timespan preceding the mainshock for which the pre-event seismicity rate significantly exceeds the background rate (Figures 2 and 3). Estimated foreshock durations for the 30 sequences range in length from 3 to 35 days, with a median of 16.6 days (Table S2). The duration estimates are limited in their precision by the uncertainty in the background rate and the temporal averaging required to compute the observed event rate. However, with nominal uncertainties of order 1 day, they still provide a useful measure of the temporal extent of elevated foreshock activity.

The foreshock sequences are diverse in their spatiotemporal evolution. Many of the longer-duration sequences are earthquake swarms that have been previously documented in select regions of southern California (Zhang & Shearer, 2016). A number of mainshocks are preceded by burst-like foreshock sequences near the mainshock hypocenter in the days and hours leading up to the event, while still others have a more diffuse and widespread elevation in seismicity rate (Figure 3). Likewise, there are some notable instances of systematic linear migration in foreshocks toward the mainshock hypocenter, but this behavior is not universally observed (Figure S4). Indeed, these sequences exemplify the diverse characteristics one might anticipate in complex natural fault systems.

What physical factors may account for the observed variations in foreshock activity? Figure 4 plots foreshock prevalence as a function of (a) mainshock magnitude, (b) mainshock depth, (c) mainshock mechanism type, and (d) heat flow (Blackwell et al., 2011). While we do not have a large enough sample size of mainshocks to make definitive conclusions, there are several intriguing trends. Mainshock magnitude and mechanism type do not appear to have a strong effect, though this may in part be a result of the fact that our dataset is relatively homogenous (i.e., M4 and M5 mainshocks, most of which are strike-slip events). Shallower mainshocks tend to have more foreshocks, a finding that is consistent with Abercrombie & Mori (1996) and Chen & Shearer (2016). Heat flow may also play an important role, with earthquakes in areas of higher heat flow tending to have more active foreshock sequences (see also Figure S5). These observations lend support to the notion posited by Abercrombie & Mori (1996) that foreshock occurrence may be controlled in part by the presence of small-scale heterogeneities in Earth's crust.

Two of the sequences without significant foreshock activity are within a remote part of the Eastern California Shear Zone with relatively sparse station coverage, so it is possible that smaller magnitude foreshocks in those particular sequences went undetected. Further, our significance criterion of $p < 0.01$ is conservative by design, and thus selects only the most robustly observed foreshock sequences. There are five additional sequences with $0.01 < p < 0.1$ in which the observed seismicity rates exceed the inferred background rate, but not to the extent where the physical significance of this rate increase is unambiguous. A close examination of how catalog magnitude of completeness correlates with foreshock prevalence (Figure 5) supports the notion that most if not all earthquakes may be preceded by small foreshocks, even if they are difficult to detect. Most of the mainshocks in our dataset without notable foreshock sequences occur in areas of larger magnitudes of completeness, which suggests that under optimal detection conditions foreshock prevalence would likely be higher than the 72% we observe. Still, there are several counterexamples where the catalog appears highly complete based on both the background seismicity and the triggered aftershocks, yet foreshocks remain elusive.

5 Discussion

We use a highly complete earthquake catalog to demonstrate that elevated foreshock activity is much more common than previously understood. The details of these foreshock sequences have to date been obscured by limitations in catalog completeness, even in southern California, where the SCSN maintains one of the most complete regional earthquake catalogs in the world. The prevalence of measurable foreshock activity we observe is reminiscent of laboratory experiments, where low-amplitude precursory slip events are ubiquitously observed preceding failure. In the laboratory, the statistical characteristics of these slip events can be used to predict the properties of imminent mainshocks, including their timing and slip amplitudes (Hulbert et al., 2019; Rouet-Leduc et al., 2017).

Many of the foreshock sequences we document in this study are extended in duration, lasting days to weeks on average. This observation lends some insight into the physical processes driving foreshock occurrence. As reviewed by Mignan (2014), two end-member conceptual models include the “cascade model” and the “preslip model” of earthquake occurrence. In the cascade model, foreshocks are viewed as a sequence of earthquakes each triggering one another, and eventually the mainshock, via earthquake-to-earthquake stress interactions. In contrast, the preslip model envisions foreshocks and the mainshock to both be triggered by a quasistatic loading process, rather than earthquake-to-earthquake triggering. Foreshocks sequences such as the one shown in Figure 3c, which is extended in duration but contains exclusively small magnitude events, are difficult to explain in terms of a cascade model of foreshock occurrence, since the cumulative stresses imparted by such small magnitude events would be unable to drive such a sequence. For example, a M2 foreshock imposes static stress changes of order 1 kPa at 500 m distance from the rupture, but this distance decreases to about 50 m for a M0 earthquake (Text S1 and Figure S6). Because of this, the extended, small-magnitude foreshock sequences we observe that encompass a wide spatial extent are likely more consistent with a preslip style of rupture nucleation, though we cannot rule out the importance of cascade-type triggering in all instances. Future work combining physical modeling with detailed observations may shed further light on this issue, particularly with regard to the variability in the spatial and temporal extent of individual foreshock sequences.

Despite the notable similarities with laboratory studies, the complexity observed in the real Earth will likely preclude hazard monitoring based on foreshock activity for the foreseeable future. Even within the limited study region of southern California, foreshock sequences vary substantially in duration and spatiotemporal evolution. It is important to note that in real fault systems, precursory activity is not a unique cause of elevated seismicity rates, which are more commonly observed in association with aftershock triggering. While foreshock activity may be apparent in retrospect after careful statistical analyses, identifying foreshocks in real time presents a different set of challenges that we do not attempt to address in this work. There are several instances of well-recorded mainshock events without detectable foreshocks, suggesting that the nucleation processes of individual earthquakes are diverse rather than universal in character. Nevertheless, by examining the details of earthquake activity at the finest of scales, we will improve our understanding of the physical mechanisms underlying how earthquakes get started.

Acknowledgments

The two earthquake catalogs analyzed in the manuscript are publicly available online. The QTM catalog and the SCSN catalog are both archived by the Southern California Earthquake Data Center (scedc.caltech.edu/). We use publicly available heat flow data from Blackwell et al., (2011). Our calculations use open source Python software packages, including a wrapper of original Okada (1992) code (Thompson, May 28, 2014/2019). D. Trugman acknowledges institutional support from the Laboratory Directed Research and Development (LDRD) program of Los Alamos National Laboratory under project number 20180700PRD1. We are grateful to P. Johnson, I. McBrearty, and N. Lubbers for discussions while formulating the study, and we thank two anonymous reviewers and editor Gavin Hayes for insightful comments and suggestions that improved the manuscript.

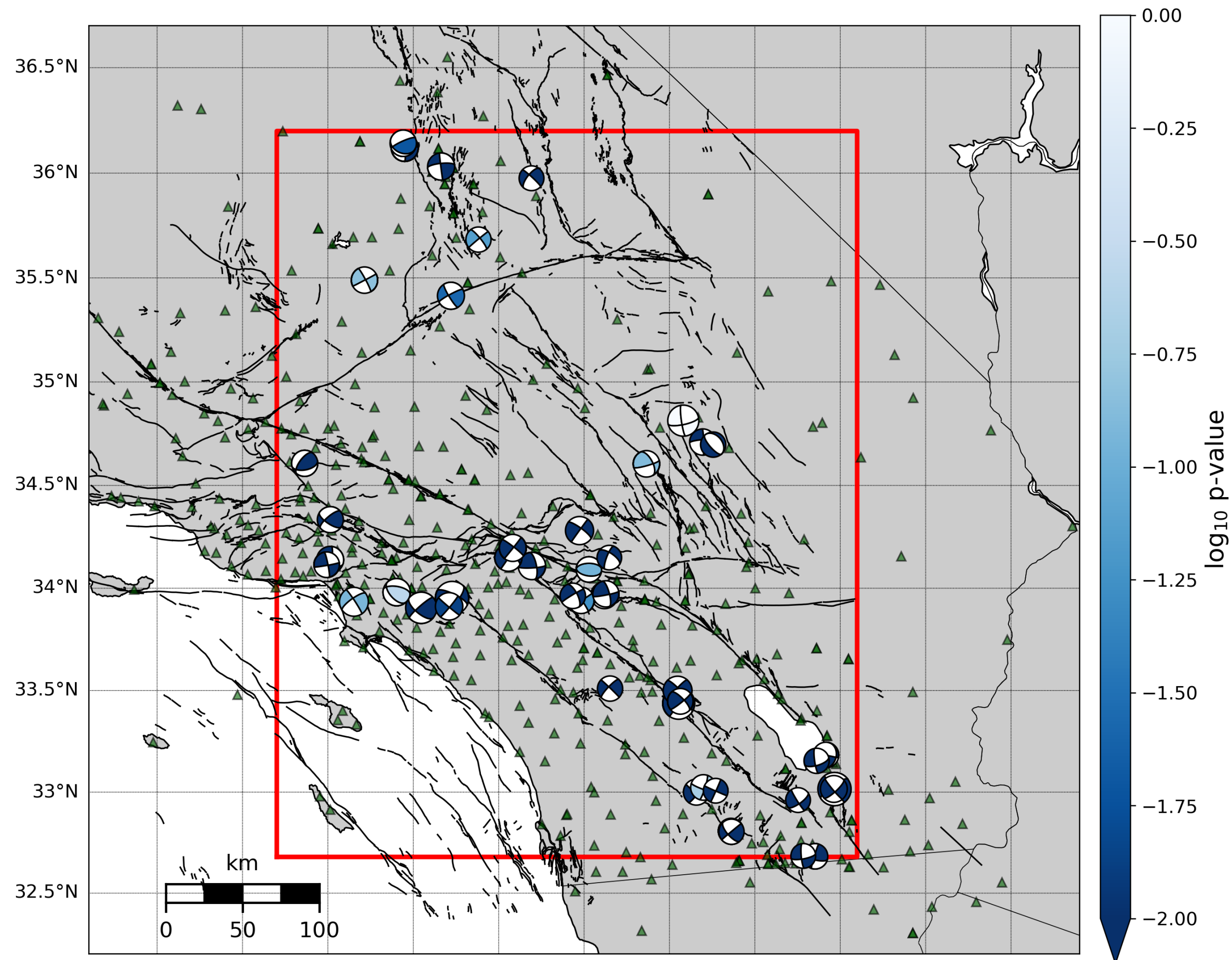

Figure 1. Foreshock sequences of 46 M4 and M5 earthquakes in southern California. The study region outlined in red – [32.68°, 36.20°] latitude and [-118.80°, -115.40°] longitude – was selected to ensure a sufficiently low magnitude of completion for detection (Figure S1). Each event is color-coded by the *p*-value measurement of foreshock activity described in the text, with lower *p*-values (darker colors) indicating more significant activity.

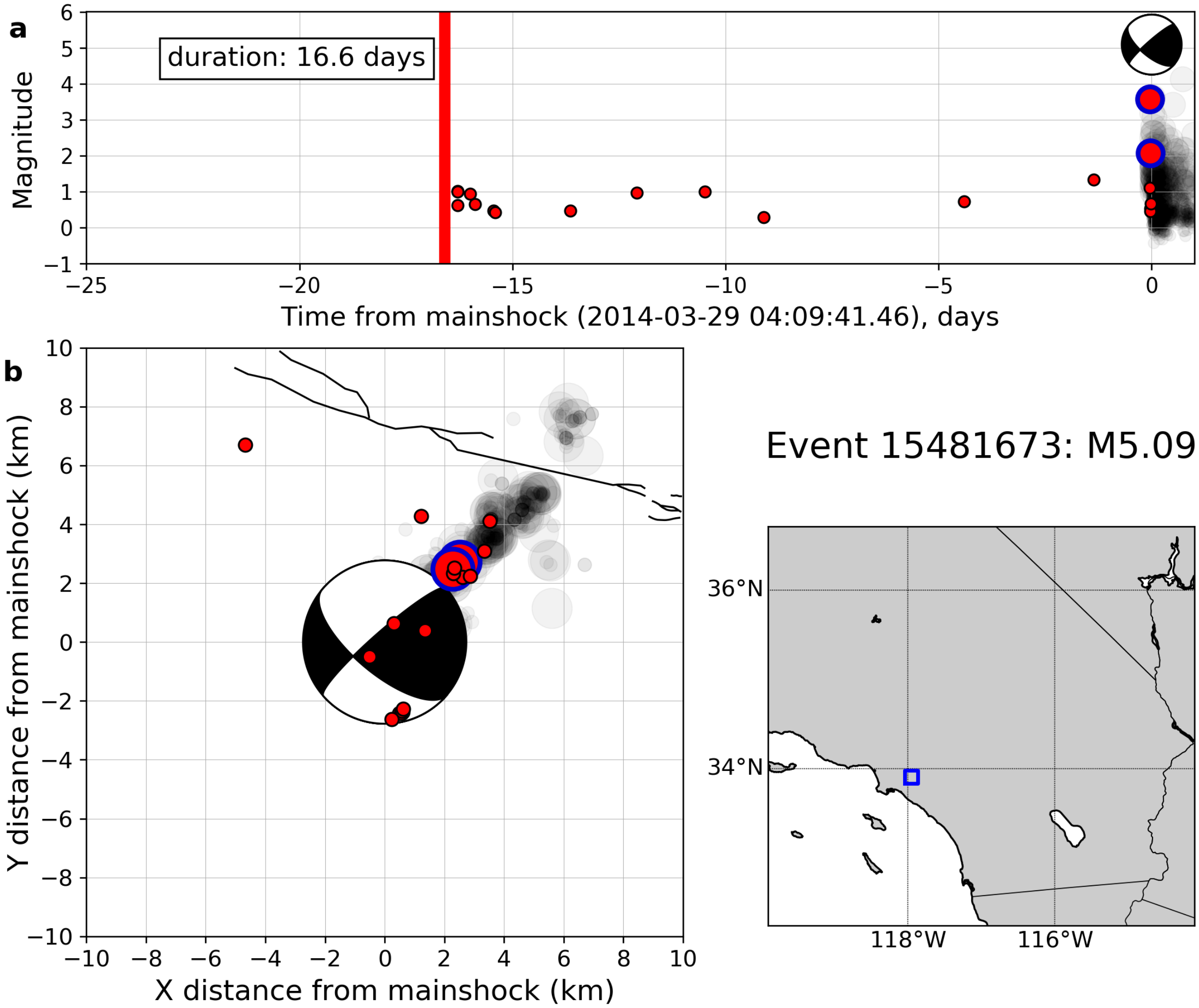

Figure 2. Foreshock sequence of the M5.09 La Habra earthquake occurring during March 2014. (a) Earthquake magnitude versus time for events within a 10 km region of the mainshock. Large circles with solid blue lines denote events listed within the SCSN catalog, while small circles denote newly detected events listed by the QTM catalog. The inferred foreshock duration of 16.6 days is denoted with a vertical red line. (b) Map view of the sequence and its location within southern California.

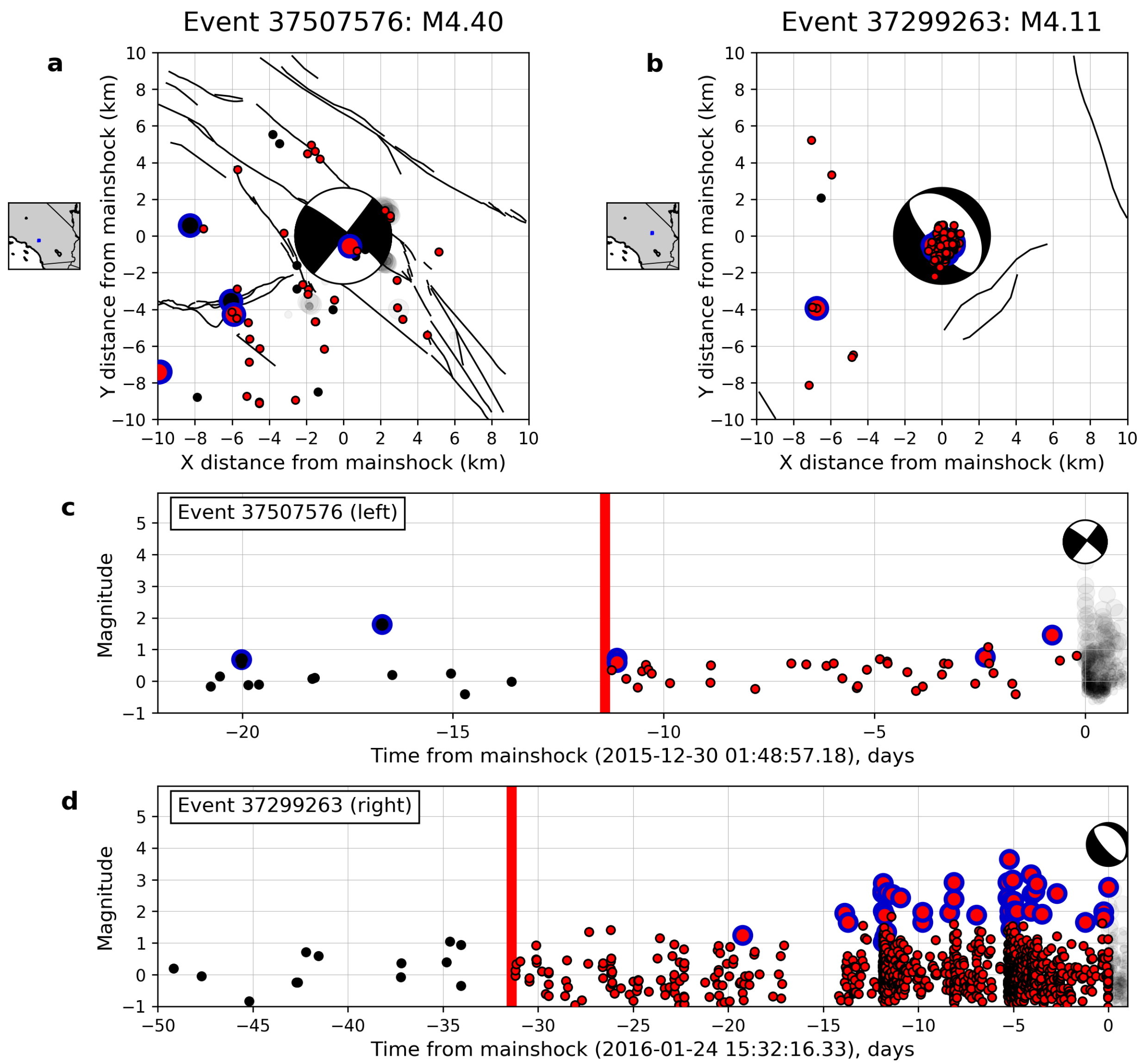

Figure 3. Diverse patterns of foreshock occurrence in southern California. Panels (a) and (b) show map view representations of two distinct foreshock sequences, one (a) with an extended period of elevated seismicity rate surrounding the mainshock hypocenter, and the other (b) with several highly localized bursts of seismicity preceding the mainshock. Red circles denote events following the estimated foreshock duration (red line), while black circles denote events preceding this. Large circles with solid blue lines denote events listed within the SCSN catalog, while small circles denote newly detected events listed by the QTM catalog. Panels (c) and (d) plot event magnitude versus time for these sequences.

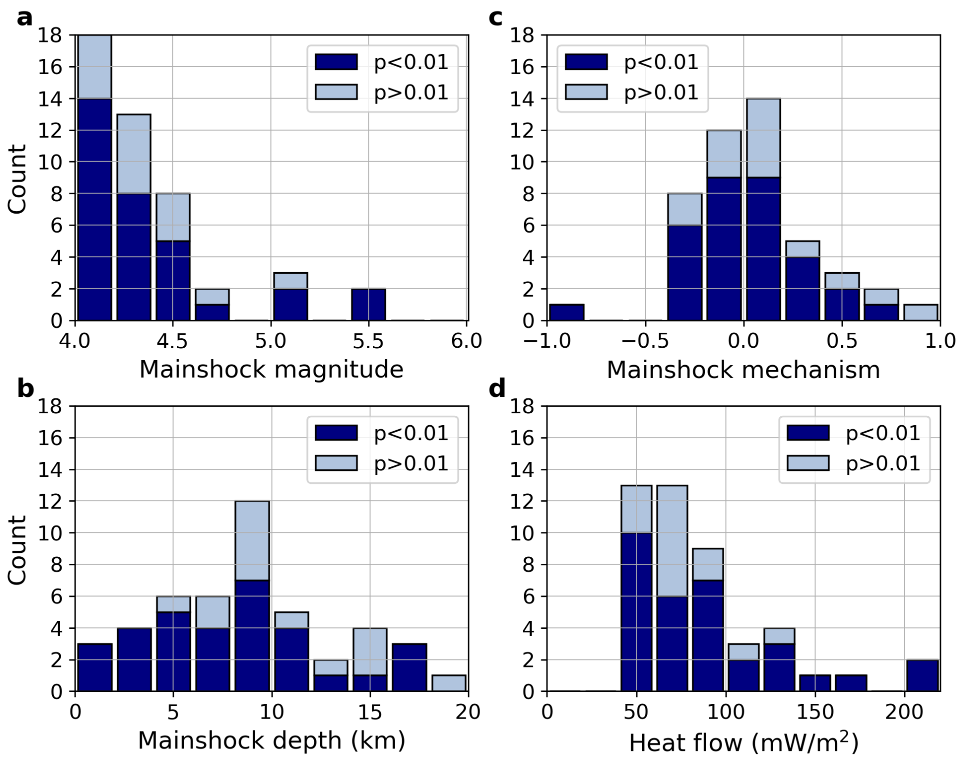

Figure 4. Relationship between foreshock prevalence and (a) mainshock magnitude, (b) mainshock depth, (c) mainshock mechanism type, and (d) heat flow (Blackwell et al., 2011). Mechanism type (c) is defined based on the listed rake value and normalized to a [-1,+1] scale, where -1 is pure normal faulting, 0 is pure strike-slip faulting, and +1 is pure reverse faulting (e.g., Chen & Shearer, 2016). In panel (d), the two earthquakes with heat flow values > 200 mW/m^2 are shifted to the rightmost bin in the plot for visual clarity, otherwise they would be to the right of the listed x-axis scale.

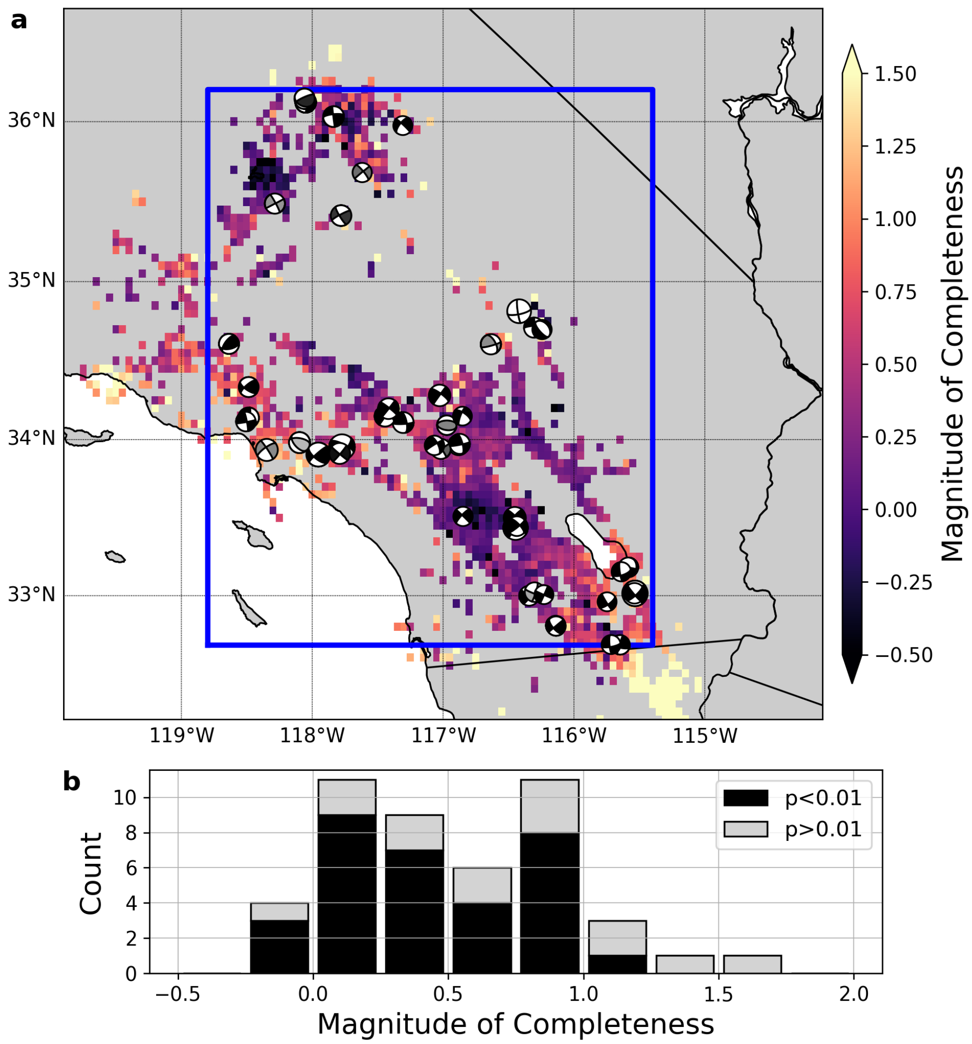

Figure 5. Relation between observed foreshock prevalence and magnitude of compleness, M_c (a) Map of spatially varying M_c, calculated using the goodness-of-fit test (Wiemer & Wyss, 2000) at the 95% confidence level. Mainshocks are marked with their slip mechanisms, with lower *p*-values (darker colors) indicating more significant foreshock activity. (b) Histogram showing the relation between local magnitude of completion and *p*-value. Most of the sequences with $p >$ 0.01 have local $M_c > 0.5$.

References

Abercrombie, R. E., & Mori, J. (1996). Occurrence patterns of foreshocks to large earthquakes in the western United States. *Nature*, *381*(6580), 303–307. https://doi.org/10.1038/381303a0

Ampuero, J.-P., & Rubin, A. M. (2008). Earthquake nucleation on rate and state faults - Aging and slip laws. *Journal of Geophysical Research*, *113*(B1). https://doi.org/10.1029/2007JB005082

Baker, J. W. (2013). An introduction to probabilistic seismic hazard analysis. *White Paper Version 2.0*, 1–79.

Blackwell, D., Richards, M., Frone, Z., Batir, J., Ruzo, A., Dingwall, R., & Williams, M. (2011). *Temperature-At-Depth Maps For the Conterminous US and Geothermal Resource Estimates* (GRC Transactions 35 No. GRC1029452). Dallas, TX: SMU Geothermal Laboratory. Retrieved from https://www.osti.gov/biblio/1137036

Bolton, D. C., Shokouhi, P., Rouet-Leduc, B., Hulbert, C., Rivière, J., Marone, C., & Johnson, P. A. (2019). Characterizing Acoustic Signals and Searching for Precursors during the Laboratory Seismic Cycle Using Unsupervised Machine Learning. *Seismological Research Letters*, *90*(3), 1088–1098. https://doi.org/10.1785/0220180367

Bouchon, M., Durand, V., Marsan, D., Karabulut, H., & Schmittbuhl, J. (2013). The long precursory phase of most large interplate earthquakes. *Nature Geoscience*, *6*(4), 299–302. https://doi.org/10.1038/ngeo1770

Brodsky, E. E. (2006). Long-range triggered earthquakes that continue after the wave train passes. *Geophysical Research Letters*, *33*(15). https://doi.org/10.1029/2006GL026605

Chen, X., & Shearer, P. M. (2013). California foreshock sequences suggest aseismic triggering process. *Geophysical Research Letters*, *40*(11), 2602–2607. https://doi.org/10.1002/grl.50444

Chen, X., & Shearer, P. M. (2016). Analysis of Foreshock Sequences in California and Implications for Earthquake Triggering. *Pure and Applied Geophysics*, *173*(1), 133–152. https://doi.org/10.1007/s00024-015-1103-0

Dieterich, J. (1994). A constitutive law for rate of earthquake production and its application to earthquake clustering. *Journal of Geophysical Research*, *99*(B2), 2601. https://doi.org/10.1029/93JB02581

Dodge, D. A., Beroza, G. C., & Ellsworth, W. L. (1996). Detailed observations of California foreshock sequences: Implications for the earthquake initiation process. *Journal of Geophysical Research: Solid Earth*, *101*(B10), 22371–22392. https://doi.org/10.1029/96JB02269

Efron, B., & Stein, C. (1981). The Jackknife Estimate of Variance. *The Annals of Statistics*, *9*(3), 586–596. https://doi.org/10.1214/aos/1176345462

Ellsworth, W. L., & Bulut, F. (2018). Nucleation of the 1999 Izmit earthquake by a triggered cascade of foreshocks. *Nature Geoscience*, 1. https://doi.org/10.1038/s41561-018-0145-1

Freed, A. M. (2005). Earthquake triggering by static, dynamic and postseismic stress transfer. *Annual Review of Earth and Planetary Sciences*, *33*(1), 335–367. https://doi.org/10.1146/annurev.earth.33.092203.122505

Freed, A. M., & Lin, J. (2001). Delayed triggering of the 1999 Hector Mine earthquake by viscoelastic stress transfer. *Nature*, *411*(6834), 180–183. https://doi.org/10.1038/35075548

Gibbons, S. J., & Ringdal, F. (2006). The detection of low magnitude seismic events using array-based waveform correlation. *Geophysical Journal International*, *165*(1), 149–166. https://doi.org/10.1111/j.1365-246X.2006.02865.x

Gomberg, J., & Davis, S. (1996). Stress/strain changes and triggered seismicity at The Geysers, California. *Journal of Geophysical Research*, *101*(B1), 733. https://doi.org/10.1029/95JB03250

Hainzl, S., Scherbaum, F., & Beauval, C. (2006). Estimating Background Activity Based on Interevent-Time Distribution. *Bulletin of the Seismological Society of America*, *96*(1), 313–320. https://doi.org/10.1785/0120050053

Hauksson, E., Stock, J., Hutton, K., Yang, W., Vidal-Villegas, J., & Kanamori, H. (2011). The 2010 Mw 7.2 El Mayor-Cucapah Earthquake Sequence, Baja California, Mexico and Southernmost California, USA: Active Seismotectonics along the Mexican Pacific Margin. *Pure and Applied Geophysics*, *168*(8–9), 1255–1277.

Hulbert, C., Rouet-Leduc, B., Johnson, P. A., Ren, C. X., Rivière, J., Bolton, D. C., & Marone, C. (2019). Similarity of fast and slow earthquakes illuminated by machine learning. *Nature Geoscience*, *12*(1), 69. https://doi.org/10.1038/s41561-018-0272-8

Hutton, K., Woessner, J., & Hauksson, E. (2010). Earthquake Monitoring in Southern California for Seventy-Seven Years (1932-2008). *Bulletin of the Seismological Society of America*, *100*(2), 423–446. https://doi.org/10.1785/0120090130

Johnson, P. A., Ferdowsi, B., Kaproth, B. M., Scuderi, M., Griffa, M., Carmeliet, J., et al. (2013). Acoustic emission and microslip precursors to stick-slip failure in sheared granular material. *Geophysical Research Letters*, *40*(21), 5627–5631. https://doi.org/10.1002/2013GL057848

Jones, L., & Molnar, P. (1976). Frequency of foreshocks. *Nature*, *262*(5570), 677. https://doi.org/10.1038/262677a0

Kilb, D., Gomberg, J., & Bodin, P. (2000). Triggering of earthquake aftershocks by dynamic stresses. *Nature*, *408*(6812), 570–574. https://doi.org/10.1038/35046046

King, G. C. P., Stein, R. S., & Lin, J. (1994). Static stress changes and the triggering of earthquakes. *Bulletin of the Seismological Society of America*, *84*(3), 935–953.

Kong, Q., Trugman, D. T., Ross, Z. E., Bianco, M. J., Meade, B. J., & Gerstoft, P. (2019). Machine Learning in Seismology: Turning Data into Insights. *Seismological Research Letters*, *90*(1), 3–14. https://doi.org/10.1785/0220180259

Koper, K. D., Pankow, K. L., Pechmann, J. C., Hale, J. M., Burlacu, R., Yeck, W. L., et al. (2018). Afterslip Enhanced Aftershock Activity During the 2017 Earthquake Sequence Near Sulphur Peak, Idaho. *Geophysical Research Letters*, *45*(11), 5352–5361. https://doi.org/10.1029/2018GL078196

Lin, J., & Stein, R. S. (2004). Stress triggering in thrust and subduction earthquakes and stress interaction between the southern San Andreas and nearby thrust and strike-slip faults. *Journal of Geophysical Research: Solid Earth (1978–2012)*, *109*(B2).

Lubbers, N., Bolton, D. C., Mohd-Yusof, J., Marone, C., Barros, K., & Johnson, P. A. (2018). Earthquake Catalog-Based Machine Learning Identification of Laboratory Fault States and the Effects of Magnitude of Completeness. *Geophysical Research Letters*, *45*(24), 13,269-13,276. https://doi.org/10.1029/2018GL079712

Marone, C. (1998). Laboratory-Derived Friction Laws and Their Application to Seismic Faulting. *Annual Review of Earth and Planetary Sciences*, *26*(1), 643–696. https://doi.org/10.1146/annurev.earth.26.1.643

Marsan, D., Helmstetter, A., Bouchon, M., & Dublanchet, P. (2014). Foreshock activity related to enhanced aftershock production. *Geophysical Research Letters*, *41*(19), 6652–6658. https://doi.org/10.1002/2014GL061219

Meng, X., & Peng, Z. (2014). Seismicity rate changes in the Salton Sea Geothermal Field and the San Jacinto Fault Zone after the 2010 Mw 7.2 El Mayor-Cucapah earthquake. *Geophysical Journal International*, *197*(3), 1750–1762. https://doi.org/10.1093/gji/ggu085

Mignan, A. (2014). The debate on the prognostic value of earthquake foreshocks: A meta-analysis. *Scientific Reports*, *4*, 4099. https://doi.org/10.1038/srep04099

Ogata, Y. (1988). Statistical Models for Earthquake Occurrences and Residual Analysis for Point Processes. *Journal of the American Statistical Association*, *83*(401), 9–27. https://doi.org/10.1080/01621459.1988.10478560

Reasenberg, P. A. (1999). Foreshock occurrence before large earthquakes. *Journal of Geophysical Research: Solid Earth*, *104*(B3), 4755–4768. https://doi.org/10.1029/1998JB900089

Ross, Z. E., Rollins, C., Cochran, E. S., Hauksson, E., Avouac, J.-P., & Ben-Zion, Y. (2017). Aftershocks driven by afterslip and fluid pressure sweeping through a fault-fracture mesh. *Geophysical Research Letters*, *44*(16), 2017GL074634. https://doi.org/10.1002/2017GL074634

Ross, Z. E., Trugman, D. T., Hauksson, E., & Shearer, P. M. (2019). Searching for hidden earthquakes in Southern California. *Science*, eaaw6888. https://doi.org/10.1126/science.aaw6888

Rouet-Leduc, B., Hulbert, C., Lubbers, N., Barros, K., Humphreys, C. J., & Johnson, P. A. (2017). Machine Learning Predicts Laboratory Earthquakes. *Geophysical Research Letters*, *44*(18), 2017GL074677. https://doi.org/10.1002/2017GL074677

Seif, S., Zechar, J. D., Mignan, A., Nandan, S., & Wiemer, S. (2019). Foreshocks and Their Potential Deviation from General Seismicity. *Bulletin of the Seismological Society of America*, *109*(1), 1–18. https://doi.org/10.1785/0120170188

Shearer, P. M., & Lin, G. (2009). Evidence for Mogi doughnut behavior in seismicity preceding small earthquakes in southern California. *Journal of Geophysical Research: Solid Earth*, *114*(B1). https://doi.org/10.1029/2008JB005982

Shelly, D. R., Beroza, G. C., & Ide, S. (2007). Non-volcanic tremor and low-frequency earthquake swarms. *Nature*, *446*(7133), 305–307. https://doi.org/10.1038/nature05666

Stein, R. S. (1999). The role of stress transfer in earthquake occurrence. *Nature*, *402*(6762), 605–609. https://doi.org/10.1038/45144

van Stiphout, T., Zhuang, J., & Marsan, D. (2012). Seismicity declustering. *Community Online Resource for Statistical Seismicity Analysis*, *10*, 1.

Tape, C., Holtkamp, S., Silwal, V., Hawthorne, J., Kaneko, Y., Ampuero, J. P., et al. (2018). Earthquake nucleation and fault slip complexity in the lower crust of central Alaska. *Nature Geoscience*, 1. https://doi.org/10.1038/s41561-018-0144-2

Thompson, B. (2019). *MATLAB and Python wrappers of the Okada Green's functions.: tbenthompson/okada_wrapper*. Fortran. Retrieved from https://github.com/tbenthompson/okada_wrapper (Original work published May 28, 2014)

Velasco, A. A., Hernandez, S., Parsons, T., & Pankow, K. (2008). Global ubiquity of dynamic earthquake triggering. *Nature Geoscience*, *1*(6), 375–379. https://doi.org/10.1038/ngeo204

W. Goebel, T. H., Schorlemmer, D., Becker, T. W., Dresen, G., & Sammis, C. G. (2013). Acoustic emissions document stress changes over many seismic cycles in stick-slip experiments. *Geophysical Research Letters*, *40*(10), 2049–2054. https://doi.org/10.1002/grl.50507

Wells, D. L., & Coppersmith, K. J. (1994). New empirical relationships among magnitude, rupture length, rupture width, rupture area, and surface displacement. *Bulletin of the Seismological Society of America*, *84*(4), 974–1002.

Wiemer, S., & Wyss, M. (2000). Minimum Magnitude of Completeness in Earthquake Catalogs: Examples from Alaska, the Western United States, and Japan. *Bulletin of the Seismological Society of America*, *90*(4), 859–869. https://doi.org/10.1785/0119990114

Yoon, C. E., O'Reilly, O., Bergen, K. J., & Beroza, G. C. (2015). Earthquake detection through computationally efficient similarity search. *Science Advances*, *1*(11), e1501057. https://doi.org/10.1126/sciadv.1501057

Zhang, Q., & Shearer, P. M. (2016). A new method to identify earthquake swarms applied to seismicity near the San Jacinto Fault, California. *Geophysical Journal International*, *205*(2), 995–1005. https://doi.org/10.1093/gji/ggw073